

SILVER NANOPARTICLES SYNTHESIS. BIOREDUCTION WITH GALLIC ACID AND EXTRACTS FROM *CYPERUS ROTUNDUS L*

C. NICHITA^{a, b}, AL-BEHADILI F. MIKHAILEF^a, E. VASILE^{*c},
I. STAMATIN^a

^aUniversity of Bucharest, Faculty of Physics, 3Nano-SAE research center 405
Atomistilor str., PO Box MG-38, Bucharest-Măgurele, Romania,

^bNational Institute for Chemical – Pharmaceutical Research and Development, 112
Vitan Avenue, 031299, Bucharest, Romania

^cPolitehnica University of Bucharest, 313 Splaiul Independentei, Bucharest,
Romania

Silver ions chemical reduced in AgNPs proved to be inappropriate for medical applications; some of the reagents have a high level of toxicity. Green synthesis removes these barriers by using the plant extracts rich in phytochemicals with high bioreduction capacity. The investigations are focusing on therapeutic effects and lesser related to the bioreduction mechanisms- phytochemical composition characterized by global parameters: total phenol content (TPC), total flavonoid content (TFC), total antioxidant capacity (TAC). TPC and TFC are measured by comparison with the gallic acid and a flavonoid (ex quercetin), respectively. Understanding their bioreduction mechanisms is useful to have a comparison criterion for each plant extract, such as TPC/TFC-ratio. In this respect, are studied the bioreduction activity for gallic acid using Pourbaix diagram, microspeciation, surface plasmon resonance, and Mie scattering, zeta potential, kinetics parameters derived from UV-vis spectroscopy and DLS. At the end are presented the kinetics parameters for the extracts from *Cyperus rotundus L.*, a plant with a high impact in phytotherapy. In introduction are summarized several keypoints, support for the understanding of the bioreduction kinetics.

(Received March 7, 2020; Accepted April 21, 2020)

Keywords: Silver nanoparticles, Green synthesis, Polyphenols, Herbal extract, Gallic acid, *Cyperus rotundus L.*, Bioreduction kinetics, UV-vis spectroscopy, Zeta potential

1. Introduction

Nanoparticles in diverse size, shapes and structures, organic and inorganic, are providing a wide spectrum for medicine to conceive new therapeutic and diagnostic agents. The aim is to find new solutions to the unsolvable diseases [1, 2, 3, 4]. Most of them are using for the drug delivery, medical devices and imaging. Regarding to the metallic nanoparticles, silver nanoparticles (AgNPs) are the most studied due to their biocompatibility and as remedy for bacterial, viral, fungal infections. Advances in green synthesis increased bioavailability and area of applications covering: bio-labeling, biomarkers, sensors [5, 6, 7], food packaging & composites [8, 9, 10, 11, 12], environmental (wastewater treatment, air pollution [13, 14, 15, 16]), dietary supplements, formulations for transdermal, oral use to name few.

The action mechanisms: when they are settling on the bacterial cells release silver ions that damage the respiratory chain, DNA, in one word the cell machinery. By comparison is like a Trojan horse for the infectious agents. However, the silver ions action on the human cells is not well understood. Their side effects (toxicity, accumulation in organs) show some biological and environmental risks. The last decades brought more information related to the action mechanisms of the AgNPs. It was suggested that AgNPs have a high affinity to bind on the proteins of the cell walls of bacteria, damaging the cell membranes [17, 18, 19, 20]. In aqueous biological media Ag

* Corresponding author: eugeniuvasile@yahoo.com

ions are released from AgNPs, pass into the cell, inactivate the metabolic processes and damage DNA [21], leading to the cell's death. Therefore, silver ions interrupt the redox processes involved in the respiratory chain. The reduced form, Ag^0 , has no effect [22]. Hereafter are summarized the main findings

- *Antibacterial activity.* Silver ions- inhibit the redox processes in the respiratory chain (electron transport, membrane permeability, proton transfer) and damage DNA. Ag^0 – has no direct effect but can modify the charge shielding, Debye length, the membrane potential when is solvated into the cell plasma.

- *The bioactivity enhancers.* AgNPs – decorated with antibiotics proved high efficiency in the bactericidal activity. For each couple AgNPs-antibiotics is an optimum ratio for the silver ion release rate and enhance the antibiotic potential [21]. The couple AgNPs-antibiotics are the most advanced products already implemented in the therapeutically chains [23, 24];

- *Concentration.* An optimum concentration of 10^{-9} - 10^{-6} mol/L is effective for the silver ions activity [21, 25, 26] to damage the respiratory chain. The excess use lead to the argyria;

- *Size, shapes, the surface energy and charge.* 1) Shapes. AgNPs with spherical shape is less active than prismatic shapes. In the prismatic shapes, corners and edges have high energy to release silver ions by comparison with spheroidal shapes. 2)Size. AgNPs with sizes under 100 nm contain 10^4 - 10^5 atoms [27, 28]. The size affects the intracellular and extra-cellular behavior. AgNPs less than 80nm can penetrate the cell membranes [29]. At lower dimensions (<10nm) cause cytoplasmatic leakage without the nucleic acid damage [30]. To maximize the bactericidal effect is to attach AgNPs on the cell membranes which cause maximum damage and induce reactive oxygen species in cytoplasm leading to the cell death [31, 32];

- *Poisoning and toxicology.* Silver ions are poisoned if appropriate anions are present in the biological fluids such chlorine, nitrates, phosphates. Also, pH can reduce the silver ions activity. Toxicological profile cover dose limit, maximum concentration, size, shapes on the human cells and organs [33, 34];

- *Bacterial resistance.* Excessive use of AgNPs lead to the development of the bacteria resistance against the ionic silver penetration. Bacteria continuous adapt by specific mechanisms becoming more resistant therefore, AgNPs-antibiotics decrease their efficiency ([21], and references in this citation).

Silver ions: reduction vs bioreduction

The wet chemistry uses the reduction route with electron donor reagents, some of them with toxic potential: sodium borohydride (NaBH_4) [35], citrate [36], polyols [37, 38], glucose & starch [39, 40, 41], alcohols [42]. The reducing agents containing carboxylic groups have the role of capping and stabilizer against oxidation [36]. The reduction agents with hydroxyl groups (alcohol, glucose, polyols) need pH compensation higher than 10 to initiate the reduction reaction [42, 43, 44]. Surfactants: Polyvinyl pyrrolidone (PVP), Tween, polyacrylic acids, some polymers with low molecular weight. They control the growth rate and aggregation [45]. Etching reagents. Hydrogen peroxide [36] and bromine compounds (KBr) [46] etch preferential crystallographic planes and spherical particles turn into some prismatic and triangular with surface plasmon resonance shifted to 450-600 nm.

The bioreduction route fulfills the green chemistry requirements: environmentally benign solvent, reducing and stabilizing reagents with high biocompatibility [47]. The plant extracts are the best suitable solutions. Rich in polyphenols and flavonoids compounds, their carboxylic and hydroxylic groups are both reducers, stabilizers, and capping agents for AgNPs [48]. On the other hand, the plant extracts have a great therapeutic value and a high capacity to reduce reactive oxygen species. The new nanoarchitecture AgNPs-plant extracts will unify both therapeutically properties in a synergistic way [48, 49]. They could fight more effectively to the bacterial infectious by diverse mechanisms decreasing the bacterial resistance [50]. Recently was devised a new type of surface engineering cell by functionalizing with AgNPs – so called “cyborg” cells [51]. That is a new way to develop bacteria, viruses, cells, functionalized with AgNPs – plant extract to fight against various bacterial or viral infections. To date, the bioreduction efficiency and therapeutically potential are extensively reviewed: [52]- general, antimicrobial [53, 54], antiviral [55], antifungal [56], anticancer [57, 58].

In a concise summary: 1) AgNPs used in excess or, in combination with antibiotics, can increase bacterial resistance. They develop immuno-resistance receptors to stop membrane penetration and reduce silver ions to a neutral state; 2) AgNPs-plant extract is an alternative to this effect. AgNPs-plant extracts enhance the potential to fight against pathogens; 3) Ag-ions bio-reduced with the plant extracts is a green synthesis method offering broad spectrum in biocompatibility-bioavailability; 4) AgNPs-size and shapes: the charge of the capping agents are controlling the rate of the silver ions release and generation of reactive oxygen species to damage membrane and the respiratory chain. The size and shape derive from the phytochemical composition; therefore, it is not necessary to use another oxidant such as hydrogen peroxide; 5) Each complex AgNPs- plant extract cover a specific therapeutic spectrum.

Almost all researches related to the Ag-ions reduction with the plant extracts focus on the size, shapes, and tests related to the anti-microbial, antiproliferative applications, to name a few. The plant extracts require phytochemical analysis, a very complicated procedure, and time-consuming. Additionally, morphology, shapes, size analyzed with SEM, TEM, XRD, FT-IR, or Raman bring information related to the AgNPs structure and the capping agent binding. A correlation phytochemical composition- silver ions bioreduction mechanisms do not yet exist. The phytochemical composition is evaluated by three global parameters: total phenolic content (TPC), total flavonoid content (TFC), total antioxidant capacity (TAC). They are using in evaluating the reducing capacity of the reactive oxygen species (known as free radical scavenger) or the bioreduction power as ligands. TPC and TFC evaluate the content of the plant extracts in the equivalent of gallic acid and a flavonoid (ex. quercetin), respectively.

To our knowledge, there is no investigation related to the kinetic mechanisms and connection with TPC and TFC. Therefore, a model for the silver ions bioreduction with gallic acid and flavonoids could help understand how each plant extract fit with AgNPs. This contribution deal with gallic acid bioreduction mechanisms. Multiple aspects are brought from electrochemistry, chemistry, and physics to understand how the couple silver ions- gallic ion species concur to a new useful AgNPs- coated with them. With Pourbaix diagram and ionization constant, solubility constant are shown conditions for alkalization and some criteria for seeding using silver clustering, growth and AgNPs stabilizing. SPR and Mie scattering – wavelength at maximum absorbance are used for the size measurements comparison with hydrodynamic size from DLS and zeta potential for AgNPs stability. Also, are established the kinetics behavior, dependence of $[Ag^+]/[GA]$ ratio. At the end these results are analyzed kinetics of the plant extract from *Cyperus rotundus* L.

This plant is well recognized in Asian Pharmacopoeia with high therapeutic potential. Some arguments are bellow summarized

In the plant world, *Cyperaceae* family has quite different therapeutic properties already used by the traditional medicines. In this family, *Cyperus rotundus* L., a mesophyte plant, has in flowers, leaves, stems, and rhizomes phytochemicals used as remedy in anti-inflammatory, anti-depressant, antipyretic, analgesic, anti-arthritis, and antiemetic for dysentery [59]. Recently, the extracts were used as remedy in Central Nervous System disorders: epilepsy, depression and inflammatory disorders, Alzheimer's disease [60, 61, 62, 63, 64, 65, 66, 67, 68, 69, 70, 71]. Phytochemical screening found polyphenols, terpenoids, quinones, glycosides and flavonoids to name a few [72, 73, 74]. Representatives in *Cyperus* spp. are cyperaquinones [75, 76] found mainly in the essential oil extracts. The first report on the Ag^+ - bioreduction proposes a mechanism where cyperaquinone (ketone-enol tautomerization) but there is no phytochemical screening [77]. In rhizomes are found components rich in polyphenols and flavonoids, essential oils.

2. Experimental part

2.1. Materials, equipment, methods

Chemicals and reagents. Silver nitrate ($AgNO_3$), sodium hydroxide (NaOH), gallic acid (99.5%), quercetin (99.8%), Mili-Q water. Total phenolic content: Folin-Ciocalteu reagent and method [78]. Total flavonoid content: reagents and solutions prepared as in [79].

Cyperus rotundus L.: dried rhizomes (source: Abu al-Khasib, Basra county, Iraq).

Equipment. Spectrophotometer UV-Vis, Jasco, V-570 (operated with 1nm resolution for wavelength) standard cuvette, 1cm optical path for the surface plasmon resonance measurements, total phenolic and flavonoid content, the bioreduction kinetic of the silver ions. The absorbance of the AgNPs consists of two components derived from scattering cross section area and absorption cross section area. The last describes the absorption band from surface plasmon resonance (SPR) due to the collective excitation of the electron gas (A_{abs}) [39, 87]. SPR absorption has a high molar extinction ($\epsilon \sim 3 \times 10^{11} \text{ M}^{-1} \text{ cm}^{-1}$) [96, 97]:

$$A_{abs} = -\log \frac{I}{I_0} = \epsilon c l \quad (1)$$

I , I_0 - the radiation intensities through cuvette, l - optical path, c -AgNPs concentration (mol/L). A realistic estimation for concentration supposes ultralow dilutions or very thin path length. In addition, the molecular extinction depends of the nanoparticle size (their cross-section area, absorption and scattering from Mie scattering). Therefore, the absorbance has a complex composition: the common feature is the wavelength coincidence where SPR and Mie scattering have the same value at maximum absorption. The only measurable parameter is the wavelength at maximum absorption and correlation with the size SEM/TEM measurements (see section 3.2) can give a useful calibration curve. Mie scattering software was used to estimate size vs wavelength at maximum absorbance (nanocomosix.com, [80]) for AgNPs bioreduced with gallic acid at concentrations 0.3÷6 μM .

For kinetics measurements at time less than 10 min was used spectrometer UV-vis, ocean optics (USB HR-4000) and software spectragryph (<https://www.ffmpeg2.de/spectragryph/>) in standard configuration (cuvette 1ml, 1cm optical path) optical stand holder with 4-way fiber optics connectors.

Zetasizer Nano ZS (Malvern Instruments Ltd.), for size distribution and zeta-potential (ZP) measurements. The average size, D_h (hydrodynamic diameter) was measured in DLS-mode with backscattering detection at 173° , laser wavelength 633nm. The suspension viscosity was measured with vibro-viscometer SV-10. Standard deviation (SD) was derived from Polydispersity index: $PDI = (SD/D_h)^2$. ZP was measured with universal cell kit, 1 mL volume. Each sample is recorded at the same concentration in DLS and ZP.

Software for gallic acid microspeciation vs pH: ChemAxon, chemicalize plugins (chemaxon.com).

2.2. *Cyperus rotundus* L.- aqueous extraction, characterization

Extraction. Rhizomes of *Cyperus rotundus* L. are ground and sieved (40 mesh sieve). 5g powder was collected and transferred in 50 mL Mili-Q water. The mixture was heated at 50°C for 30 min under stirring (details in [81]). The solution was filtered in the follow sequences: gross with Whatman no.4, fine with filters 1 and 0.2 microns and finally with funnel -frit glass, porosity 1-5% (under vacuum). The solution was centrifugated at 500g to remove any residue and the supernatant stored at 4°C. The extraction yeald: 8.6% (supernatant dried under vacuum at 40°C, 4 days)

Total phenol content (TPC). Folin -Ciocalteu method [82, 83], reference Gallic acid (3 hydroxyls and 1 carboxyl group in structure). Total phenolic content in equivalent Gallic acid: TPC= 842±/ 13 ppm, (4.95 μM equivalent GA)

Total flavonoid content: (TFC). AlCl_3 -method [79, 84, 85], reference quercetin (flavanol with 5 hydroxyl groups in structure). Total flavonoid content in equivalent quercetin: TFC= 264±/ 12 ppm (0.91 μM equivalent quercetin)

Ratio TPC/TFC ~5.44, useful to appreciate the bioreduction capacity, type of stabilizer and capping agent (contribution carboxylic groups vs hydroxyls).

2. 3. Bioreduction of silver ions to AgNPs.

The extract from *Cyperus rotundus* L. contains phenols 4.95 μM equivalent GA and flavonoids 0.91 μM equivalent quercetin. Total, 5.86 μM equivalent phyto-reductant found in 5g dried extract. For comparison with gallic acid are prepared solutions with concentrations, 0.3÷6 μM and

investigated in the first stage the optimum value for AgNPs with highest ZP. In the second stage is investigated the bioreduction mechanisms. Further is analyzing the bioreduction behavior of the plant extract.

In this respect, are prepared 1mM AgNO₃ in Milli-Q water, with pH=11 (using 0.1M NaOH) [86] and gallic acid solution with concentration from 0.3 to 6μM. In 50 mL 1mM AgNO₃ are added 2mL from each gallic solution (dropwise with stirring at RT). Concentration ratio [Ag⁺]/[GA] is shown in table 1. The reduction of Ag⁺ to Ag⁰ was confirmed by the color change of the solution from colorless, yellow-pale, yellow to yellow-intense. Silver nanoparticles formation was also confirmed by recording SPR absorption spectrum.

3. Results and discussions

3.1. Bioreduction mechanisms

Silver ions are reduced by Gallic acid only in alkaline aqueous solutions with pH >10 or the molar ratio [NaOH]/[Ag⁺]_~10 [44]. Also, in citrate or glucose-based systems without addition of NaOH, the reduction reaction cannot happen [87]. There are two strategies in the silver reduction: 1) when are using citrates as a stabilizer then silver ions are reduced via strong reductant such as NaBH₄ to form AgNPs-seeds, and then citrate ions control the growth. Similar effects have a series of carboxylic acids [36] (see dashed circle figure 1); 2) When the phenolic acids are reductant and stabilizing agent then it is necessary the alkalization of the silver salt solution. A useful tool to understand the bioreduction mechanism with gallic acid is the Pourbaix diagram (figure 1) in correlation with the ionic speciation counted based on pK_a of the gallic acid moieties (figure 2). Pourbaix diagram [88] gives a straightforward understanding of the chain of reactions. Silver-H₂O diagram is drawn using data from [89]. At pH~ 11 the stable phase Ag₂O in coincidence with oxygen evolution (dashed line) reaction lead to the reduction with OH⁻ ions (potential range 0.3-0.6V). The band at ~270-280nm in UV-vis spectrum (low absorption) is assigned to the metastable clusters [Ag₄(OH)₂]⁺ [90], formed in the reaction:

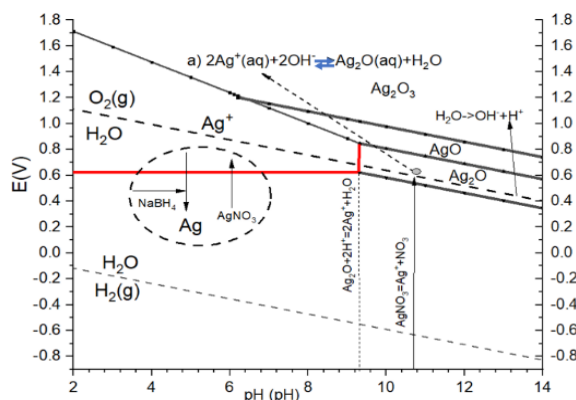
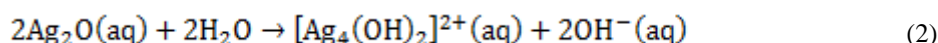
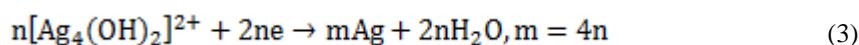


Fig. 1. Silver-H₂O -Pourbaix diagram, Potential E vs-pH. Dashed lines correspond to the water in thermodynamic equilibrium with oxygen and hydrogen at 1bar. Red lines are Ag⁺/Ag and Ag⁺/Ag₂O equilibrium counted for 1mM AgNO₃. Dashed circle corresponds to the reduction with NaBH₄, pH<9. At pH~11 silver ions are in the first stage reduced to Ag₂O (aq) reaction (a). The reverse reaction is solubilization and Ag₂O- oxidation.



Additionally, this comes from a high solubility of Ag₂O in water. The solvation constant for Ag₂O/AgOH has value pK_s=-7.7 [91]. That shows a high solvation capacity and strengthens the formation of silver clusters from silver hydroxides as an intermediate route, eq (2, 3 and a Fig. 1). Silver clusters are reduced by the molecules that release electrons in an oxidation reaction:



and grow to form AgNPs,



followed by stabilization and capping with the molecular ions from the gallic acid. It is easy to observe that for each 4Ag^+ need one gallic acid and $\frac{1}{2}\text{NaBH}_4$ (Fig. 1) or maybe lesser. Anyhow, the ratio $[\text{Ag}^+]/[\text{GA}]$ is an important feature in the reduction/bioreduction kinetics. The gallic acid releases two electrons and two protons when $\text{pH} > 9$ (figure 2). The oxidation potentials for $-\text{OH}$ (positions 3 and 4) $\sim 0.35\text{V}$, and for $-\text{OH}$ (position 5) and carboxyl is $\sim 0.65\text{V}$ [92, 93]. In inset (figure 2) is shown the gallic acid oxidation to quinone form via two steps reaction. As the oxidation potentials for gallic acid are appropriate with the reduction potentials for Ag_2O , they form at molecular level a redox microcouple, and the reactions proceed autocatalytic. Microspecies 3,4 prevent Ag_2O -precipitation and stabilize the silver clusters. In the first stage, AgNPs-nucleation, the silver clusters co-aggregate to form critical stable nuclei (nucleation stage I, figure 7). Further, they grow and are stabilizing by the gallic acid moieties and hydroxyls (stage II). The zeta potential increases due to silver ions attachment (Fig. 6). When the potential reaches $\sim 0.65\text{V}$, that is appropriate for the carboxyl group oxidation, and lead to the attachment on the AgNPs surface, as stabilizer, capping agent and charge compensation, respectively. This happen in the stage III where the chemical potentials of the silver ions in solution and on the AgNPs surface are equals.

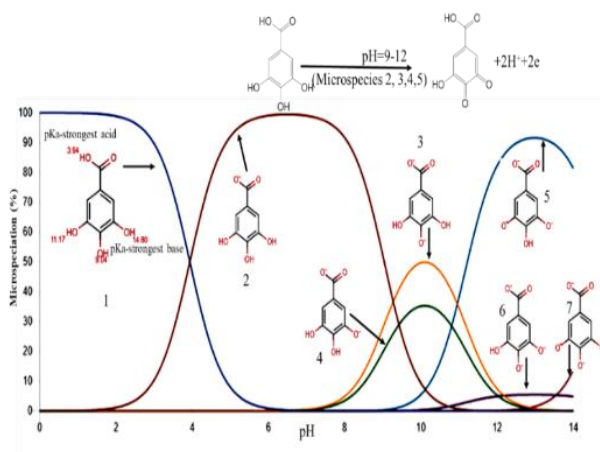


Fig. 2. Gallic acid. Concentration of the molecular ions (Microspecies)- pH. At $\text{pH}=9-12$ Gallic acid is oxidized to the molecular ions 3,4,5. The reduced forms, quinones, takes place via $2e-2\text{H}^+$ transfer (see inset). software chemAxon, plug-in, chemicalize (www.chemaxon.com).

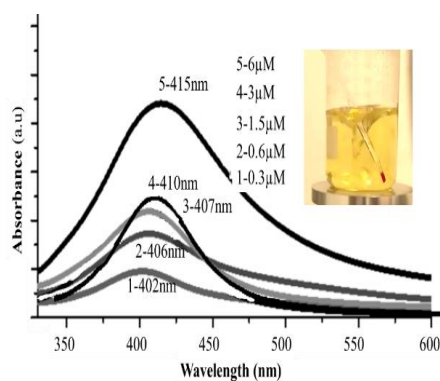


Fig. 3. UV-vis spectra recorded at 10min for Ag^+ bioreduction with Gallic acid: 1mM AgNO_3 solution with pH=11 and 2mL Gallic acid with 0.3-6 μM concentration. $[\text{Ag}^+]/[\text{GA}]=367, 183, 73, 37, 18$.

The electrical double layer (Stern layer [94], Fig. 6) is made of gallic acid monolayer interconnected with hydrogen bonds on the positions 3&5. ZP-values are measured on the slipping layer. Based on these assumptions and observations from correlation Pourbaix diagram- microspeciation of the gallic acid then the bioreduction mechanisms should proceed as an autocatalytic reaction in the first stages nucleation and growth continued with stabilizing AgNPs by gallic acid molecules on their surface. Moreover the surface plasmon resonance should not be strong influenced by the bioreductant that being an intrinsic property of the conductive nanoparticles and their size [90] (in hypothesis the electron density is constant). UV-vis spectra recorded for silver bioreduced with gallic acid at concentrations from 0.3 to 6 μM (Fig. 3) shows an increased absorption and the maximum of the wavelength slightly moved to higher values.

The colour of the solutions after 10 min changes from yellow pale to yellow intense. DLS measurements: hydrodynamic size and zeta potential are presented in Table 1.

Table 1. AgNPs-GA, data measured after 10 min. Hydrodynamic size (D_h), Z-potential (ZP), λ_{max} from UV-vis spectra (figure 3), d -calculated [93]with calibration curve Fig. 5, Mie- simulation using refractive index (nanocomposix.com).

[GA], μM	$[\text{Ag}^+]/$ [GA]	D_h (nm),	ZP (mV)	λ_{max} (exp)	d (nm) [93]	Mie λ_{max}	RI
0.3	367	53 \pm 37	-21.4	402	23	398	1.3311
0.6	183	48 \pm 31	-22.0	406	31	404	1.3322
1.5	73	45 \pm 31	-22.4	407	32	404	1.3355
3	37	46 \pm 32	-26.4	410	37	410	1.3408
6	18	45 \pm 18	-29.8	415	43	416	1.3922

RI- refractive index: $1.33*(1-x)+1.73*x$, $x=[\text{GA}]/[\text{Ag}^+]$, 1.73- RI for gallic acid. Standard deviation was calculated using PDI

The sizes of the nanoparticles, d , are estimated with data from [93] and the fitting equation, Fig. 5, using values measured in figure 3, $\lambda_{\text{max}}(\text{exp})$. For each d , are calculated, λ_{max} , from Mie scattering simulation with appropriate refractive index (RI) and in assumption 1 monolayer gallic acid. $[\text{Ag}^+]/[\text{GA}] = \text{No silver ions} / \text{gallic acid molecule}$.

As expected at low concentrations the spectrum has a broad shape with low absorption and narrows with wide tail towards red wavelength. At higher concentration the spectrum is asymmetric (positive skewness). The nanoparticle size, calculated from $\lambda_{\text{max}}(\text{exp})$, increases with the gallic acid concentration. Hydrodynamic size decreases with the concentration. It can be supposed there is a transition from a diffusive layer to a strong Stern layer made of single molecular gallic acid (see Fig. 6): due to solvation there is a wide diffusive shell of water molecules with gallic acid interconnected by hydrogen bonding at low concentration (ex 0.3 μM).

Mie scattering simulation give several key-points. For example, $d=43\text{nm}$ and 1 monolayer of gallic acid and RI =1.3922 the maximum wavelength, $\lambda_{\text{max}}\sim 416\text{nm}$ appropriate with the experimental value. From RI result $[\text{Ag}^+]/[\text{GA}]\sim 23$. At higher RI ~ 1.53 , the wavelength does not change ($[\text{Ag}^+]/[\text{GA}]\sim 7$). It can be assumed that at $[\text{Ag}^+]/[\text{GA}] < 23$ AgNPs reach maximum coverage with gallic acid.

ZP increases in absolute value from 21 to $\sim 30\text{mV}$. Worth noted if the dilutions are in buffers or physiological solutions that is meaningless due to disturb the potential at sliding layer (Nernst potential). Additionally, the rule of thumb, if $\text{ZP} < -30\text{mV}$ means good stability, $\sim -20\text{mV}$ – short term stability, higher than -5mV takes place aggregation [95] (applicable for low molecular stabilizer/ capping agent, for other macromolecules it should takes in account the steric effects).

At low gallic acid concentrations AgNPs have a good stability but the differences between real size ($\sim 23\text{ nm}$ estimated from maximum wavelength absorption) and hydrodynamic size ($\sim 53\text{nm}$) could come from very low concentration of capping agents interconnected with hydrogen

bonds (Fig. 6). They could form a large electrical double layer with the slipping plane at several nanometer apart from the AgNPs surface. Also, at high gallic acid concentration ($\sim 6\mu\text{M}$) hydrodynamic diameter and SPR diameter have appropriate value and ZP= -29.8mV . That means a very thin shell layer made of gallic acid molecules (Stern layer). It can be concluded that the optimum ratio for bioreduction is $[\text{Ag}^+]/[\text{GA}]\sim 18$ in agreement with Mie scattering simulations.

3.2. Kinetics ($t > 10\text{min}$)

The experimental conditions were divided in two parts: 1) Growth for times >10 min where are studied the stabilization dynamic of AgNPs, and 2) nucleation, growth and stabilizing AgNPs- if the bioreduction with gallic acid is autocatalytic.

In the first set of experiments are analyzed samples with $6\mu\text{M}$ GA in 1mM AgNO_3 , $\text{pH}=11$ (Table 1). In Fig. 4 are shown the absorption spectra recorded from 10 min to 220 min. For each time are measured, λ_{max} , peak-area, and ZP. Peak area gives id relate to the oscillator strength of the SPR. ZP- increases up to -31 - 32 mV, confirming that AgNPs are more stable and reach a maximum coverage with gallic acid.

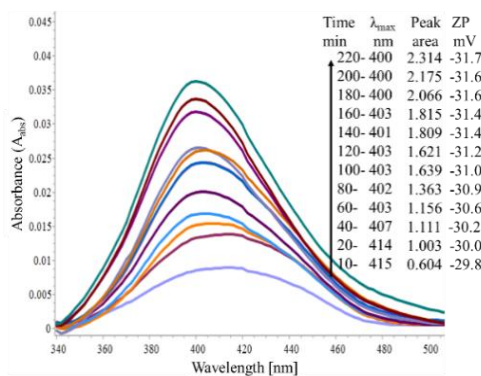


Fig. 4. Absorption spectra for 1mM Ag ions reduced with $6\mu\text{M}$ Gallic Acid ($[\text{Ag}^+]/[\text{GA}]=18$).

In Fig. 5 are shown the size vs growth time: λ_{max} vs $t(\text{exp})$ – right axis & upper axis. On the left-axis- is the calibration curve $\lambda_{\text{max}}(d)$ -based on the references included in figure 5. The color change vs time is inserted: from yellow pale to yellow intense

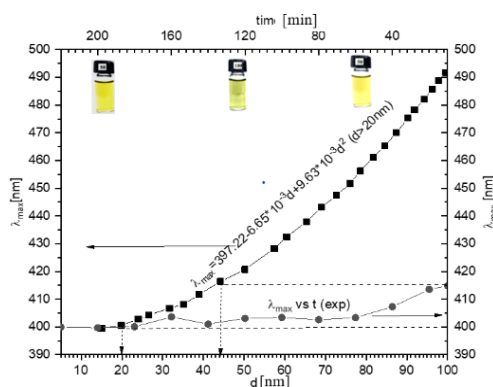


Fig. 5. Relationship between maximum absorption, λ_{max} and AgNPs size. Data collected from [96 .97 , 98] for the calibration curve $\lambda_{\text{max}}(d)$.

The wavelength shift from 415 nm to 400 nm and the peak area increases from 0.604 to 2.314 . Zeta potential also increases with the bioreduction time up to -31.7 mV.

During growth AgNPs decrease in size from 45 nm to $\sim 20\text{nm}$ (figure 5). Also, the color changes from yellow pale to yellow intense. As expected AgNPs size should grow; instead, they

are reducing. It must take in account that the silver ions concentration is constant (1mM). From the mass balance result that during biosynthesis are changing only size and the concentration of the nanoparticles.

In this respect, in the last stage the AgNPs exchange silver ions to and from solution until the chemical potentials reach to minimum and the ZP to maximum value. Therefore, for a certain initial concentration and for a fixed ratio $[Ag^+]/[bioreductant]$ there is a minimum size. The AgNPs are in continuous dynamics until all Ag^+ are consumed from solution.

Fig. 6 a suggests the competitive mechanisms dissolution -growth processes until the chemical potential of the silver ions from solution and from ANPs are equilibrated and the stabilizing agents reach the maximum coverage.

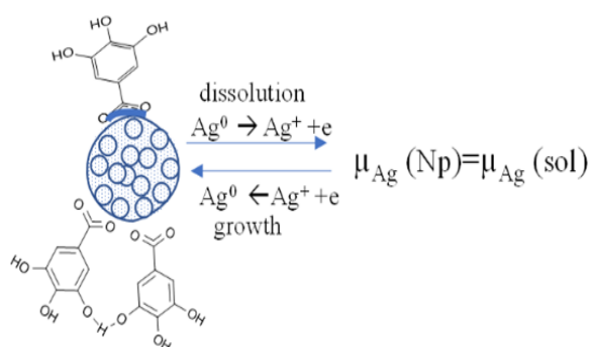


Fig. 6. a – a model dissolution-growth by which Ag^+ are reciprocal transferred between NPs until chemical potential reaches to equilibrium.

(Stern layer & diffusive layer). The larger sizes are reducing and the concentration of smaller sizes increase. Ideally, a stable AgNPs-solution with capping agents stabilized will contain a monomodal size distribution. In solvent the Ag^+ - concentration = 0.

Fig. 6 b sketches the stabilizing agent formation around of AgNPs (microspecies 5, Fig. 2) when the surface reaches to -0.65 V and the hydrogen bonding between the quinone forms. The carboxylic groups are oxidizing and compensate the surface charge by bonding with Ag^+ (-Ag-O-C-O-Ag-).

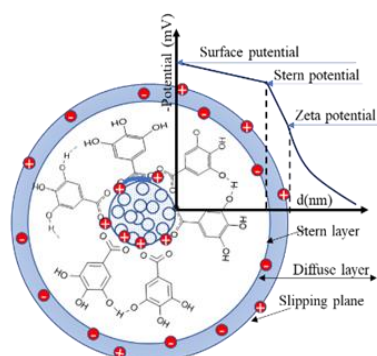


Fig. 6. b Electrical double layer formation by a monolayer of gallic acid (Stern layer) and a diffusive layer- ZP- measured at slipping plane.

The stabilizing layers is equivalent with the Stern layer. The quinone forms are interconnected by hydrogen bonds. Transition from Stern layer to the diffusive layer and the charge compensation is made of a mixture water - gallic acid microspecies. The slipping plane define hydrodynamic size, the separation AgNPs - solvent. ZP is that value for a stable nanoparticle in equilibrium with solvent.3.3

3.3. Kinetics (t<10min)

The study of absorbance during bioreduction under 10 min describes the first stages from nucleation to growth (I+II) and gives information about the type of kinetics. Stage III is a transition to the stabilizing and capping with the molecular microspecies of the gallic acid, as shown above, takes more than 100 min (Fig. 5).

The kinetics describe the nuclei formation and their growth mediated by bioreductant. With the assumptions outlined in section 3.1 (eq 2-4), the nucleation proceeds from clusters $[Ag_4(OH)_2]^{2+}$ reduced by microspecies resulted from the gallic acid at pH > 9 (see figures, 1 & 2).

The proposed kinetics is autocatalytic one. In this respect, the AgNPs concentration vs. time should have a sigmoidal profile [99]. As the absorbance $A \sim c$ in the assumption, the molecular extinction is constant in figure 7 are shown the measurements carried out at 415 nm vs. time up to 500 s. The spectrometer configuration and associated software carried out the kinetic in the optical cuvette at a fixed wavelength (415nm). Figure 7a shows a sigmoidal growth with three regions– nucleation(I), growth (II), stabilization (III). Nucleation: governed by the equations 2-4. The bioreduction takes place via the electron-proton donors from the gallic acid microspecies. Growth: the critical nuclei (nanoparticles, stable thermodynamic) grow by a continuous influx of silver ions from the solution until they reach a positive potential $\sim 0.65V$, threshold for the carboxylic groups' oxidation at pH>10. At this stage, the nanoparticles are stabilizing, as shown in III- Fig. 7. A plot of the reduced absorbance $a = A(t)/A(500)$ recorded at 415 nm (Fig. 7 right) allows estimating the time constant for which the silver nanoparticle concentration reaches 50% (or silver ions are 50% converted in AgNPs). In other words, after ~ 175 s, 50% of silver ions are converted in AgNPs by an autocatalytic process (equation written in Fig. 7 right).

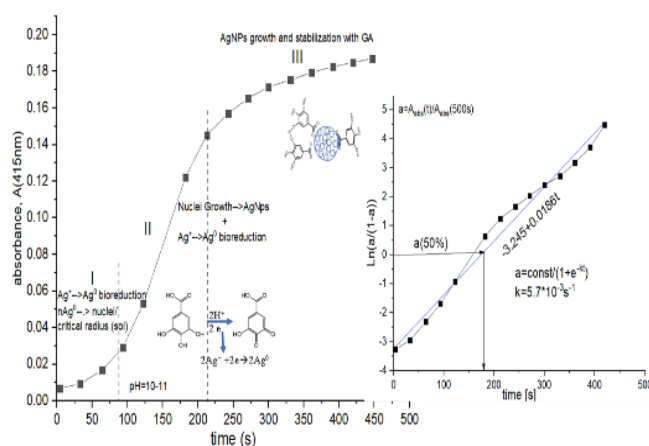


Fig. 7. Kinetics curve derived from absorbance $A(415nm)$ vs time. (left). Right- plot of the reduced absorbance, a , as $\ln(a/(1-a))$ vs time.

3.4. Bioreduction with extract from *Cyperus Rotundus L*

The extract from *Cyperus rotundus L.* contains equivalent of phenolic acids and flavonoids with ratio TPC/TFC ~ 5.44 (section 2.2) beside other phytochemicals which can speed up or slow down the bioreduction kinetics. Few studies are found with the flavonoid bioreduction. For example quercetin in alkaline solution (pH $\sim 7.5-11$) [100] produces AgNPs with SPR absorption band at ~ 415 nm $[Ag^+]/[quercetin] \sim 400$. Other flavonoids have a very low bioreduction capacity.

The quercetin microspeciation correspond to the oxidizing OH-groups similar with gallic acid [101]. Therefore, some of flavonoids may slow down the bioreduction kinetics and move the absorption band to higher values. In this respect without new calibration curves for size the main instruments remain DLS and SEM/TEM. In Fig. 8 are shown the bioreduction kinetics with the aqueous extract from *Cyperus rotundus L.* At a first sight, for $t < 10$ min could not identify any

change. At time > 10min the absorbance increases very slow and color of the solution changes from yellow to green dark and red dark.

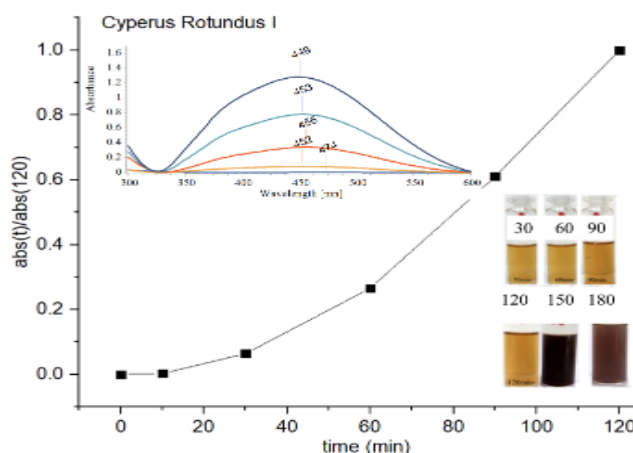


Fig. 8 Bioreduction of silver NPs with *Cyperus rotundus L-* extract.

The maximum of absorbance was recorded at ~450-456 nm. The reduced absorbance has a quite different behavior by comparison with the gallic acid. The earlier report [100] shows that the flavonoids have a sluggish bioreduction kinetics and lead to AgNPs with bigger size (mainly quercetin). Other flavonoids (naringenin) has no bioreduction activity. In addition, if pH > 8 the yield of AgNPs is less. Even though flavonoids have high antioxidant activity their bioreduction activity is quite different than polyphenols. Therefore, a small content of flavonoids drastically changes kinetics, as well pH must be correlated with TPC/TFC ratio to reduce Ag₂O formation and precipitation. In table 2 it sees that the hydrodynamic size is relatively bigger than values found for gallic acid with the same evolution but more sluggish than that observed in Fig. 5. Zeta potential still remains in the range where the nanoparticles have a good stability.

Table 2. DLS characteristics of AgNPs – biosynthesis with aqueous extract from *Cyperus Rotundus L.*

time (min)	D _h (nm)	ZP (mV)
10	67±13	-27
30	64±11	-29
60	60±14	-27
90	63±13	-28
120	56±17	-28

These facts can be explained taking into account the structural differences: flavonoids (some of them) have an extended conjugated system than polyphenols.

Even though they can contain the same number of hydroxyl groups which provide high bioreductive activity the difference consists in two step- processes by comparison with flavonoids the oxidation takes place by complex multi-steps leading to a lower rate of kinetics. Obviously, the steric effects have an important contribution.

4. Conclusions

This contribution carried out a literature survey related to the AgNPs synthesis using chemical and bio-reductants originated from the phytochemical compounds, today “green synthesis.” Some key points are identified to drive the biosynthesis of AgNPs using extracts from plants (total phenol & flavonoid content, pH, phytochemical composition). Some reports approached the kinetics of bioreduction by focusing on the size, stabilization and capping. A kinetic model was proposed using Pourbaix diagram, microspeciation and Mie scattering simulation. Then this model was applied to the gallic acid, the reference molecule for TPC estimation. A collection of data from literature wavelength- size where SPR of AgNPs reach the maximum absorption allowed us to have a calibration curve.

The autocatalytic conversion governs the kinetics of transformation, Ag⁺ in AgNPs, and their stabilization takes place by developing an electrical double layer. Gallic acid and the silver ions can be oxidized, respectively reduced if they form a microcouple with appropriate values of the potentials. Finally, is studied if TPC/TFC ratio changes the kinetics of the bioreduction. The study was carried out on *Cyperus Rotundus* L, a plant with a broad therapeutic spectrum but less known in the AgNPs biosynthesis. It is shown that the flavonoid content lead to a sluggish kinetics

TPC/TFC ratio could be an effective parameter to evaluate the AgNPs biosynthesis with the plant extracts.

Acknowledgments

This work was supported by a grant of the Romanian Ministry of Research and Innovation, CCCDI – UEFISCDI, project number PCCDI-76/2018 and PCCDI-40/2018. One of co-author thank to the Doctoral School in Physics, University of Bucharest for scientific and technical assistance. Contribution: Nichita & Faisal developed the concept and experimental part, E Vasile-coordinate the analysis, Stamatin- coordinate all activity during this research.

References

- [1] L. Zhang, F. X. Gu, J. M. Chan, A. Z. Wang, R. S. Langer, O. C. Farokhzad, *Clinical pharmacology & therapeutics* **83**(5), 761(2008).
- [2] W. Lin, Introduction: nanoparticles in medicine, 10407 (2015).
- [3] W. Joy, M. Zhu, Y. Yang, J. Shen, E. Gentile, D. Paolino, M. Fresta et al., *Current drug targets* **16**(14), 1671(2015).
- [4] S. K. Murthy, *International journal of nanomedicine* **2**(2), 129 (2007).
- [5] J. Yguerabide, E. E. Yguerabide, *Analytical biochemistry* **262**(2), 157 (1998).
- [6] R. G. Bai, K. Muthoosamy, F. N. Shipton, A. Pandikumar, P. Rameshkumar, N. M. Huang, S. Manickam, *RSC Advances* **6**(43), 36576 (2016).
- [7] L. Tang, C. Dong, J. Ren, *Talanta* **81**(4-5), 1560 (2010).
- [8] E. Fortunati, I. Armentano, Qi Zhou, A. Iannoni, E. Saino, L. Visai, Lars A. Berglund, J. M. Kenny. E. I. Fortunati Armentano, Qi Zhou, A. Iannoni, E. Saino, L. Visai, Lars A. Berglund, J. M. Kenny. *Carbohydrate polymers* **87**(2), 1596 (2012).
- [9] P. Kanmani, J. W. Rhim, *Food chemistry* **148**, 162 (2014).
- [10] Y. Echevoyen, C. Nerín, *Food and Chemical Toxicology* **62**, 16 (2013).
- [11] M. E. Barbinta-Patrascu, N. Badea, M. Constantin, C. Ungureanu, C. Nichita, S. M. Iordache, A. Vlad, S. Antohe, *Romanian Journal of Physics* **63**, 702 (2018).
- [12] A. Stefancu, S. D. Iancu, V. Moisoiu, N. Leopold, *Rom Rep Phys* **70**, 4 (2018).
- [13] I. S. Yunus, Harwin, A. Kurniawan, D. Adityawarman, A. Indarto, *Environmental Technology Reviews* **1**(1) 136 (2012).
- [14] K. Y. Yoon, J. H. Byeon, C. W. Park, J. Hwang, *Environmental science & technology* **42**(4),

- 1255 (2008).
- [15] T. M. Benn, P. Westerhoff, *Environ. Sci. Technol* **42**(11), 4133 (2008).
- [16] K. Bilberg, H. Malte, T. Wang, E. Baatrup, *Aquatic Toxicology* **96**(2), 159 (2010).
- [17] A. C. Burduşel, O. Gherasim, A. Grumezescu, L. Mogoantă, A. Ficai, E. Andronescu, *Nanomaterials* **8**(9), 681 (2018).
- [18] K. Mijndonckx, N. Leys, J. Mahillon, S. Silver, R. V. Houdt, *Biometals*, **26**(4), 609 (2013).
- [19] L. Wei, J. Lu, H. Xu, A. Patel, Z. S. Chen, G. Chen, *Drug discovery today* **20**(5), 595 (2015).
- [20] T. C. Dakal, A. Kumar, R. S. Majumdar, V. Yadav, *Frontiers in microbiology* **7**, 1831 (2016).
- [21] J. Y. Maillard, P. Hartemann, *Critical Reviews in Microbiology* **39**(4), 373 (2012).
- [22] G. A. Sotiriou, S. E. Pratsinis, *Environmental science & technology* **44**(14), 5649 (2010).
- [23] A. R. Shahverdi, A. Fakhimi, H. R. Shahverdi, S. Minaian, *Nanomedicine: Nanotechnology, Biology and Medicine* **3**(2), 168 (2007).
- [24] A. M. Fayaz, K. Balaji, M. Girilal, R. Yadav, P. T. Kalaichelvan, R. Venketesan, *Nanomedicine: Nanotechnology, Biology and Medicine* **6**(1), 103 (2010).
- [25] S. Silver, L. T. Phung, *J Ind Microbiol Biotechnol* **32**, 587 (2005).
- [26] S. Silver, L. T. Phung, G. Silver, *J Ind Microbiol Biotechnol*. **33**, 627 (2006).
- [27] S. Agnihotri, S. Mukherji, S. Mukherji, *RSC Advances* **4**(8), 3974 (2014).
- [28] S. Pal, Y. K. Tak, J. M. Song, *Applied and environmental microbiology* **73**(6), 1712, (2007).
- [29] X. H. N. Xu, W. J. Brownlow, S. V. Kyriacou, Q. Wan, J. J. Viola, *Biochemistry* **43**, 10400 (2004).
- [30] S. K. Gogoi, P. Gopinath, A. Paul, A. Ramesh, S. S. Ghosh, A. Chattopadhyay, *Langmuir* **22**, 9322 (2006).
- [31] M. Banerjee, S. Mallick, A. Paul, A. Chattopadhyay, S. S. Ghosh, *Langmuir* **26**, 5901 (2010).
- [32] J. R. Morones, J. L. Elechiguerra, A. Camacho, K. Holt, J. B. Kouri, J. T. Ramirez, M. J. Yacaman, *Nanotechnology* **16**(10), 2346 (2005).
- [33] L. Kvítek, A. Panacek, R. Prucek, J. Soukupova, M. Vanickova, M. Kolar, R. Zboril, *Journal of Physics: Conference Series*. **304**(1) IOP Publishing, 012029 (2011).
- [34] A. B. Lansdown, *Advances in pharmacological sciences*, ID 910686, (2010).
- [35] L. Mulfinger, S. D. Solomon, M. Bahadory, A. V. Jeyarajasingam, S. A. Rutkowsky, C. Boritz, *Journal of chemical education* **84**(2), 322 (2007).
- [36] Q. Zhang, N. Li, J. Goebel, Z. Lu, Y. Yin, *J. Am Chem Soc* **133**(46), 18931 (2011).
- [37] Y. Sun, B. Mayers, T. Herricks, Y. Xia, *Nano letters* **3**(7), 955 (2003).
- [38] P. Y. Silvert, R. Herrera-Urbina, K. Tekai-Elhsissen, *Journal of Materials Chemistry* **7**(2), 293 (1997).
- [39] V. K Sharma, R. A. Yngard, Y. Lin. *Advances in colloid and interface science* **145**(1-2), 83 (2009).
- [40] H. Wang, X. Qiao, J. Chen, S. Ding, *Colloids and Surfaces A: Physicochemical and Engineering Aspects* **256**(2-3), 111 (2005).
- [41] P. Raveendran, J. Fu, S. L. Wallen, *Journal of the American Chemical Society* **125**(46), 13940 (2003).
- [42] Z. Y. Huang, G. Mills, B. Hajek, *The Journal of Physical Chemistry* **97**(44), 11542 (1993).
- [43] K. Esumi, T. Hosoya, A. Suzuki, K. Torigoe, *Journal of colloid and interface science* **226**(2), 346 (2000).
- [44] K. Yoosaf, B. I. Ipe, C. H. Suresh, K. G. Thomas, *The Journal of Physical Chemistry C* **111**(34), 12839 (2007).
- [45] E. Izak-Nau, A. Huk, B. Reidy, H. Uggerud, M. Vadset, S. Eiden, M. Voetz, M. Himly, A. Duschl, *Rsc Advances* **5**(102), 84172 (2015).
- [46] A. J. Frank, N. Cathcart, K. E. Maly, V. Kitaev, *Journal of Chemical Education* **87**(10), 1098 (2010).
- [47] P. T Anastas, J. C. Warner, *Green Chemistry: Theory and Practice*, Oxford University Press, Inc.: New York, 1998.
- [48] S. Iravani, *Green Chemistry* **13**(10), 2638 (2011).

-
- [49] N. Tarannum, Y. K. Gautam, RSC Advances **9**(60), 34926 (2019).
- [50] N. Durán, P. D. Marcato, M. Durán, A. Yadav, A. Gade, M. Rai, Applied microbiology and biotechnology **90**(5), 1609 (2011).
- [51] S. A. Konnova, A. A. Danilushkina, G. I. Fakhrullina, F. S. Akhatova, A. R. Badrutdinov, R. F. Fakhrullin, RSC Advances, **5**(18), 13530 (2015).
- [52] H. P. Borase, B. K. Salunke, R. B. Salunkhe, C. D. Patil, J. E. Hallsworth, B. S. Kim, S. V. Patil, Applied biochemistry and biotechnology **173**(1), 1 (2014).
- [53] D. A. Mubarak, N. Thajuddin, K. Jeganathan, M. Gunasekaran, Colloids and Surfaces B: Biointerfaces **85**(2), 360 (2011).
- [54] S. Ahmed, M. Ahmad, B. L. Swami, S. Ikram, Journal of advanced research **7**(1), 17 (2016).
- [55] S. Gaikwad, A. Ingle, A. Gade, M. Rai, A. Falanga, N. Incoronato, L. Russo, S. Galdiero, M. Galdiero, International journal of nanomedicine **8**, 4303 (2013).
- [56] S. W. Kim, J. H. Jung, K. Lamsal, Y. S. Kim, J. S. Min, Y. S. Lee, Mycobiology **40**(1), 53 (2012).
- [57] D. Nayak, S. Pradhan, S. Ashe, P. R. Rauta, B. Nayak. Journal of colloid and interface science **457**, 329 (2015).
- [58] M. Rath, S. S. Panda, N. K. Dhal, Int J Plant Anim Environ Sci **4**, 137 (2014).
- [59] A. M. Peerzada, H. H. Ali, M. Naeem, M. Latif, A. H. Bukhari, A. Tanveer, Journal of ethnopharmacology **174**, 540 (2015).
- [60] A. Azimi, S. M. Ghaffari, G. H. Riazi, S. S. Arab, M. M. Tavakol, S. Pooyan, Journal of Ethnopharmacology **194**, 219 (2016).
- [61] S. H. Jung, S. J. Kim, B. G. Jun, K.T. Lee, S.P. Hong, M.S. Oh, D.S. Jang, J.H. Choi, Journal of ethnopharmacology **147**(1), 208 (2013).
- [62] M. S. Sundaram, T. Sivakumar, G. Balamurugan, Biomedicine **28**, 302 (2008).
- [63] N. A. Raut, N. J. Gaikwad, Fitoterapia **77**, 585 (2006).
- [64] S. Kilani, R. B. Ammar, I. Bouhlel, A. Abdelwahed, N. Hayder, A. Mahmoud, K. Ghedira, L. Chekir-Ghedira, Environmental Toxicology and Pharmacology **20**(3), 478 (2005).
- [65] M. Zhu, H. H. Luk, H. S. Fung, C. T. Luk, Phytotherapy Research **11**(5), 392 (1997).
- [66] S. Kilani, I. Bouhlel, R. B. Ammar, M. B. Sghair, I. Skandrani, J. Boubaker, A. Mahmoud, M. G. Dijoux-Franca, K. Ghedira, L. Chekir-Ghedira, Annals of microbiology **57**(4), 657 (2007).
- [67] S. Kilani, J. Ledauphin, I. Bouhlel, M.B. Sghaier, J. Boubaker, I. Skandrani, R. Mosrati, K. Ghedira, D. Barillier, L. Chekir-Ghedira, Chemistry & Biodiversity **5**(5), 729 (2008).
- [68] R. S. Dhillon, S. Singh, S. Kundra, A.S. Basra, Plant growth regulation **13**(1), 89 (1993).
- [69] D. K. Pal, S. Dutta, Indian J. Pharm. Sci. **68**, 256 (2006).
- [70] S. Kilani, M. B. Sghaier, I. Limem, I. Bouhlel, J. Boubaker, W. Bhourri, I. Skandrani, A. Neffatti, R. B. Ammar, M. G. Dijoux-Franca, K. Ghedira, Bioresource technology **99**(18), 9004 (2008).
- [71] J. B. Harborne, C. A. Williams, K. L. Wilson, Phytochemistry **21**(10), 2491 (1982).
- [72] K. R. Nagulendran, S. Velavan, R. Mahesh, V. H. Begum, Journal of Chemistry **4**(3), 440 (2007).
- [73] S. R. Sivapalan, P. Jeyadevan, International Journal of Pharmacology and Pharmaceutical Technology **1**(2), 42 (2012).
- [74] Z. Zhou, W. Yin, Molecules **17**(11), 12636 (2012).
- [75] R. H. Thomson, Naturally occurring quinones. Elsevier, 2012.
- [76] R. H. Thomson, Quinone: nature, distribution and biosynthesis, in: T.W. Goodwin (Ed.), Chemistry and Biochemistry of Plant Pigments, Academic Press, NY, pp. 527, (1976).
- [77] A. K. Jha, Prasad, K., Prasad, A. R. Kulkarni, Colloids and Surfaces B: Biointerfaces **73**(2), 219 (2009).
- [78] V. L. Singleton, R. Orthofer, R. M. Lamuela-Raventós. Methods in enzymology **299**, 152 (1999).
- [79] V. Dewanto, Xianzhong Wu, K. K. Adom, Rui Hai Liu. Journal of agricultural and food chemistry **50**(10), 3010 (2002).
- [80] S. J. Oldenburg, Light Scattering from Gold Nanoshells. Diss. Rice University, 2000.

-
- [81] Amita Pandey, Shalini Tripathi. *Journal of Pharmacognosy and Phytochemistry* **2**(5), (2014).
- [82] Romanian Pharmacopoea, ed. X. (1993), Bucharest, Ed. Medicala, 335, 779.
- [83] V. L. Singleton, R. Orthofor, R. M. L Raventos. *Methods Enzymol.* **299**, 152 (1999).
- [84] A. Bashir, B. Sultana, F. H. Akhtar, *Afr J Basic Appl Sci* **4**(1), 1 (2012).
- [85] Chia-Chi Chang, Ming-Hua Yang, Hwei-Mei Wen, Jiing-Chuan Chern. *Journal of food and drug analysis* **10**, 3 (2002).
- [86] G. A. Martínez-Castañón, N. Niño-Martínez, F. Martínez -Gutierrez, J. R. Martínez -Mendoza, Facundo Ruiz, *J Nanopart Res* **10**, 1343 (2008).
- [87] A. Henglein, M. Giersig, *The Journal of Physical Chemistry B* **103**(44), 9533 (1999).
- [88] M. Pourbaix, in *Atlas of Electrochemical Equilibria in Aqueous Solution*, 2nd ed., p. 394, National Association of Corrosion Engineers, Houston, TX (1974).
- [89] Paul Delahay, Marcel Pourbaix, Pierre Van Rysselberghe. *Journal of The Electrochemical Society* **98**(2), 65 (1951).
- [90] A. Henglein, *The Journal of Physical Chemistry* **97** (21), 5457 (1993).
- [91] W. Feitknecht, P. Schindler, *Pure Appl. Chem.* **6**, 125 (1963).
- [92] P. V Cherepanov, Arifur Rahim, Nadja Bertleff-Zieschang, Abu Sayeed, A. P. O'Mullane, S. E. Moulton, F. Caruso. *ACS applied materials & interfaces* **10**(6), 5828 (2018).
- [93] Abdel-Hamid Refat, Emad F. Newair, *Journal of electroanalytical chemistry* **657**(1-2), 107 (2011).
- [94] P. R Mishra, L. Al Shaal, R. H. Müller, C. M. Keck, *International journal of pharmaceutics* **371**(1-2), 182 (2009).
- [95] Thomas M Riddick. *Control of colloid stability through zeta potential*. Wynnewood, PA: Livingston, 1968.
- [96] D. Paramelle, A. Sadovoy, S. Gorelik, P. Free, J. Hobley, D. G. Fernig. *Analyst* **139**(19), 4855 (2014)
- [97] D. D Evanoff, G. Chumanov, *The Journal of Physical Chemistry B* **108**(37), 13948 (2004).
- [98] D. D Evanoff, G. Chumanov, *The Journal of Physical Chemistry B* **108**(37), 13957 (2004).
- [99] Ioana Stanciu, *Mechanism of autocatalytic reactions 2014*, Ed Lambert, ISBN: 978-3-659-64978-3.
- [100] E. A Terenteva, V. V. Apyari, S. G. Dmitrienko, Yu A. Zolotov, *Spectrochimica Acta Part A: Molecular and Biomolecular Spectroscopy* **151**, 89 (2015).
- [101] A. M. O. Brett, M. E. Ghica. *Electroanalysis: An International Journal Devoted to Fundamental and Practical Aspects of Electroanalysis* **15**(22), 1745 (2003).